TURBULENCE AND VERTICAL STABILITY IN THE CALIFORNIA CURRENT

DAVID M. HUSBY AND CRAIG S. NELSON

Pacific Environmental Group
Southwest Fisheries Center
National Marine Fisheries Service
National Oceanic and Atmospheric Administration
P.O. Box 831
Monterey, California 93942

ABSTRACT

Summaries of historical surface marine wind observations and subsurface temperature data are used to examine the seasonal and spatial characteristics of wind-generated turbulent energy production and of stability of the upper water column over the California Current region. A recent hypothesis suggests that survival of first-feeding larval anchovies, *Engraulis mordax*, depends on the aggregation of properly sized food organisms in a stable water column in the absence of strong wind-induced turbulence. A comparison of wind mixing and stability indices for regions encompassing the principal spawning grounds of the three subpopulations of northern anchovy demonstrates that peak spawning occurs during seasons and in locations associated with stable stratification, relatively low rates of turbulent energy production, and weak offshore transport (upwelling).

The average intensity of wind-generated turbulent energy production is similar during peak spawning periods in all three regions. This suggests optimum levels of turbulence and stability in the upper water column—levels that favor survival of first-feeding larvae. Although examination of mean conditions is useful in a comparative study, the average intensity of turbulent wind mixing over a spawning season is not likely to be well correlated with interannual variability in recruitment. Rather, the existence of sufficient time-space windows within which turbulence does not exceed critical values may be the relevant factor. To investigate this possibility, time series of wind-generated turbulent energy production are presented for recent periods associated with large variations in year-class strength.

RESUMEN

Para estudiar las características estacionales y espaciales de la producción de energía eólica turbulenta y la estabilidad de la columna superior de agua en la región de la Corriente de California, se emplean observaciones del viento en la superficie del mar y de temperatura subsuperficial. Ultimamente se ha planteado una hipótesis que propone que la supervivencia de las larvas de anchoveta, *Engraulis mordax*, al iniciar su

alimentación, depende del conjunto de organismos alimenticios de medida apropiada presentes en una columna de agua estable donde no existe fuerte turbulencia eólica. Una comparación de los índices de mezcla eólica y los de estabilidad de las regiones que abarcan las principales áreas de desove de las tres subpoblaciones de anchoveta del norte, muestra que el período de máximo desove ocurre en estaciones y lugares en donde la estratificación es estable, los índices de producción de energía eólica turbulenta son relativamente bajos, y la surgencia de aguas es débil.

La intensidad media de la producción de energía eólica turbulenta es igual en las tres regiones durante los períodos de máximo desove. Esto implica que existen niveles óptimos de turbulencia y estabilidad en la parte superior de la columna de agua, los cuales son propicios para la supervivencia de las larvas. Si bien un examen de las condiciones medias es útil en un estudio comparativo y es improbable que la intensidad media de la mezcla eólica turbulenta durante la estación de desove esté bien correlacionada con la variabilidad interanual en el reclutamiento. Más bien parece que el factor determinante podría ser la existencia de suficientes intervalos de tiempo y espacio, donde la turbulencia no excede valores críticos. Para investigar esta posibilidad se presentan series de tiempo de la producción de energía eólica turbulenta de etapas recientes vinculadas con importantes variaciones en la cantidad de anchoveta para cada generación.

INTRODUCTION

The concept of a "critical period" in the early life history of fishes was formulated in Hjort's pioneering studies (1914, 1926) on the year-class strength of Norwegian herring and cod stocks. The critical-period hypothesis suggests that survival of larval fish might be affected by (1) a lack of food at the time of first feeding, and (2) currents that transport larvae to areas unfavorable to further growth. The relationships of nonseasonal fluctuations in surface transport to larval survival and year-class strength have been investigated in recent correlative studies on Pacific mackerel, *Scomber japonicus*, (Parrish and MacCall 1978) and Atlantic menhaden, *Brevoortia tyrannus*, (Nelson et al. 1977). Parrish et al. (1981) have discussed the

general relationship of surface transport mechanisms to reproductive success of pelagic fishes in the California Current system. However, even where apparent linkages between surface drift conditions and stock variations have been demonstrated, larval survival is still critically dependent on food availability. Hjort emphasized the first of these two critical-period mechanisms in determining year-class strength (May 1974).

Recent laboratory and field studies by Lasker et al. (1970) and Lasker (1975, 1978) indicate that survival of first-feeding larval northern anchovies, *Engraulis mordax*, may depend on several related factors: (1) the existence of fine-scale food strata containing high concentrations of properly sized food particles, (2) the coincidence of patches of larvae with adequate patches of food, and (3) the absence of predator populations sufficient to destroy the larval patches (Lasker and Smith 1977). On the principal anchovy spawning grounds off southern California, Lasker (1978) found that stability of the water column in the upper 30 m appeared to be a necessary condition for these fine-scale food strata. From additional survey data, Lasker (1981b) concluded that stability in the upper layers of the ocean during the anchovy spawning season is prerequisite to a successful year class. Wind-generated turbulent mixing associated with storms or strong coastal upwelling events destroys the required vertical stratification and patchiness, thereby contributing to increased larval mortality, which may result in a poor year class.

The purpose of this study is to describe the spatial patterns and annual cycles of climatological indices of wind-generated turbulent energy production and vertical stability in the California Current region. Bakun and Parrish (1980) suggested that information on the normal requirements for reproductive success of pelagic fishes might be obtained by comparing environmental conditions in the spawning areas with the conditions in regions where spawning does not usually occur. In this study, we compare monthly and seasonal indices of wind-generated turbulent mixing and upper ocean stability in the principal northern anchovy spawning areas to further explore the relationship of a stable ocean to larval survival, as described by Lasker (1981a). We will examine these indices in relation to the timing and locations of spawning of the three subpopulations of northern anchovy (Figure 1). To the extent that the mechanisms in Lasker's hypothesis exert a strong control on spawning success in the three subpopulations, there should be marked similarities among the wind-mixing and stability indices in all three spawning regions along the west coast of North America.
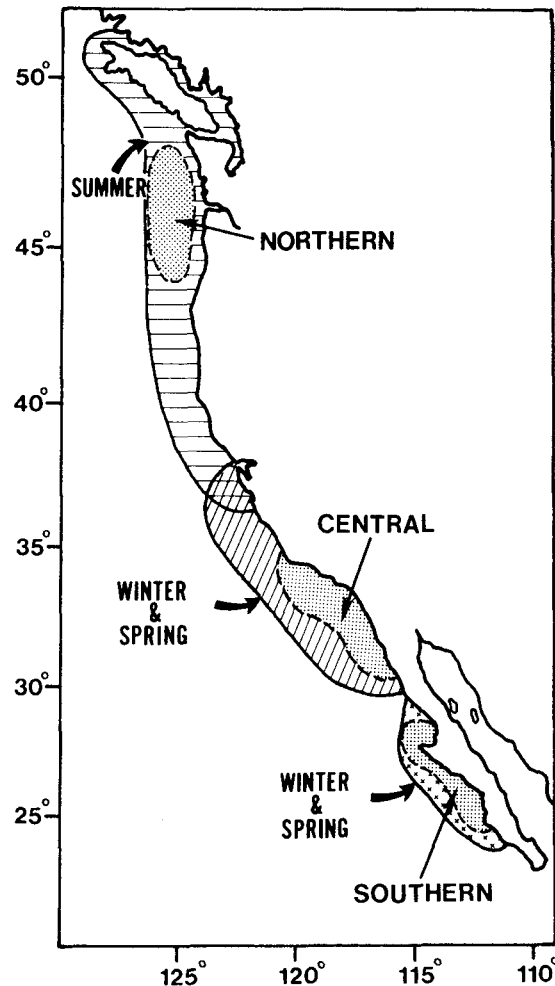

Figure 1. Geographic ranges (hatched), principal spawning areas (shaded), and seasons of the three subpopulations of northern anchovy, *Engraulis mordax*. Geographic ranges are modified from Smith and Lasker (1978) and Vrooman et al. (1981). Spawning areas have been inferred from egg and larvae distributions during the peak spawning months (Kramer and Ahlstrom 1968; Hewitt 1980; Richardson 1980).

DATA DESCRIPTION

Stability within the upper layers of the ocean is primarily determined by a balance between the net downward heat flux across the air-sea interface and turbulent mixing processes associated with wind-stirring and convective cooling. The evolution of transient and seasonal thermoclines can be predicted on the basis of the imbalance between the heat input from the atmosphere to the ocean and the intensity of turbulent wind mixing, which redistributes heat throughout the mixed layer. Strong surface heating

during extended periods of light winds can produce strong stratification and rapid transitions to shallow mixed layers (Elsberry and Garwood 1978). Atmospheric forcing associated with winter storms or strong coastal upwelling "events" can destroy the stratification in the upper layers of the water column and rapidly deepen the "well-mixed" layer. Nelson (1977) and Nelson and Husby (in press) described the climatological distributions of surface wind stress and surface heat flux over the California Current region. This study extends the previous work to include summaries of an index of wind-generated turbulent energy production associated with redistribution of heat in the upper layers of the ocean and an index of upper-layer vertical stability resulting from surface heat flux and turbulent mixing processes.

Wind Mixing

The rate at which turbulent kinetic energy of the wind is added to the upper ocean and becomes available to mix the stable thermocline layers is proportional to the third power, or "cube," of the wind speed (Niiler and Kraus 1977). The proportionality factor is not well established and must be determined empirically from laboratory measurements and field calibrations. Because our main purpose is to make intraregional and seasonal comparisons, a sufficiently accurate index of the rate of turbulent energy production can be computed from the cube of the surface wind speed. Estimated and measured surface wind speeds were obtained from the historical surface marine weather observations archived in the National Climatic Center's (NCC) Tape Data Family-11 (TDF-11). This is the same set of data used by Nelson (1977) to compute surface wind stress and wind stress curl over the California Current.

Long-term monthly and quarterly means of the cube of the scalar wind speed were computed from all available surface marine reports from 1850 to 1972 for each 1-degree square area within a geographical region extending from 20°N to 50°N and from the west coast of North America to 10 degrees of longitude offshore. The same summary grid and editing procedures described by Nelson (1977) were adopted. Winter and summer quarters were chosen to approximately coincide with the peak spawning seasons for the southern, central, and northern subpopulations of the northern anchovy, respectively. Because we are interested in characterizing wind-generated turbulence in the important nearshore spawning habitats (Brewer and Smith 1982), long-term means were also computed for several partial 1-degree coastal squares that were not included in Nelson's (1977) wind stress distributions.

The principal sources of error in climatological means based on surface wind data are associated with imprecise Beaufort wind force estimates and nonuniform distributions of data in time and space (see Nelson 1977 for a discussion of errors). These errors are accentuated by computing the cube of a scalar variable. Sampling bias is even more critical to the stability index calculations (described in the next section) for which the available data are at least one order of magnitude less than the surface weather reports. Although each of the long-term monthly 1-degree square means is independent of all other months and squares, statistical independence is less important than the ability to present characteristic spatial and temporal distributions of wind speed cubed and vertical stability in the California Current. Therefore, when contoured fields have been used to display the results, the mean distributions were machine contoured, subjectively smoothed, and recontoured to remove "bull's-eyes" associated with extreme variability and inadequate sampling. Because most of the sampling error occurs offshore, this procedure should not substantially affect the conclusions for the nearshore regions.

Vertical Stability

Vertical stability of an oceanic water column depends on the vertical distribution of density, which is a function of temperature, salinity, and pressure. A water column is stably stratified if the density increases with depth. A commonly used index of the static stability of the water column, suggested by Hesselberg and Sverdrup (1915; cited in Sverdrup et al. 1942), is proportional to the vertical gradient of sigma-t, σ_t, (the density at atmospheric pressure):

$$E' = 10^{-3} \, d\sigma_t/dz \qquad (1)$$

The total expression for stability contains additional small terms related to the vertical gradients of temperature and salinity and the adiabatic temperature change due to compressibility. However, Hesselberg and Sverdrup (1915) have shown that stability in the upper 100 m is accurately expressed by Equation (1).

The computation of sigma-t requires values of temperature and salinity as a function of depth. The numbers of hydrographic stations that include vertical profiles of both temperature and salinity, over the entire California Current region, are rather small in terms of spatial and temporal coverage. For this reason, the more extensive set of mechanical bathythermograph (MBT) observations, which provide profiles of temperature versus depth, was used to compute an index of the vertical stability of the upper water column. The use of the vertical temperature structure to approximate the stability of the upper layer is valid if density

depends primarily on temperature (i.e., little error will result in using only vertical temperature gradients to compute stability if the salinity is constant with depth or if the salinity gradients are small).

The waters flowing southward in the California Current are characterized by a shallow salinity minimum, which is due to the cool, low-salinity subarctic water mass being overrun from the west by the warmer, high-salinity subtropical water of the central Pacific anticyclonic gyre (Reid 1973). Figure 2 displays the January and June mean temperature-salinity (T-S) curves at standard depths to 500 m for three lines of 1-degree squares at 46°N, 33°N, and 27°N, respectively. The rightmost curves in each panel represent the 1-degree squares adjacent to the coast. These curves were derived from the National Oceanographic Data Center's (NODC) Station Data II file (SDII), including data to 1973.

The eastern North Pacific Ocean north of 40°N is influenced strongly by an annual excess of precipitation over evaporation, and the vertical salinity structure is characterized by a permanent halocline between 100 and 200 m (Tully 1964). Figure 2A shows this subarctic structure, particularly for the T-S curves 3 to 4 degrees of longitude offshore, where the upper 50-100 m is characterized by relatively uniform and low salinity values (32.5⁰/oo), below which there is an increase in salinity to a value of 33.8⁰/oo at 200 m. The nearshore coastal waters off the Pacific Northwest are strongly influenced by the seasonal discharge of the Columbia River drainage basin. Peak discharges during May and June produce a large plume of low-salinity water (<32.0⁰/oo) in the upper 30 m; the plume extends toward the southwest from the mouth of the Columbia River (46°N) and can be distinguished as far as 500 km from shore (Barnes et al. 1972). Although the Columbia River plume is identified by low salinities in the surface layer, the distribution of the plume has been observed to be closely approximated by the 20-m isopleth of the thermal mixed layer depth during July (Owen 1968). During winter the region of diluted surface waters extends seaward about 50 to 100 km and from about 100 km south of the mouth of the Columbia River to the Strait of Juan de Fuca.

The cool subarctic waters in the California Current are modified by lateral mixing with the subtropical water mass to the west and by upwelling along the coastal margin (Tibby 1941). The first two 1-degree squares adjacent to the coast at 33°N (Figure 2B) are representative of conditions within the Southern California Bight. The seasonal changes in the upper 75 m of the water column are primarily due to the increase in solar insolation that contributes to the for-
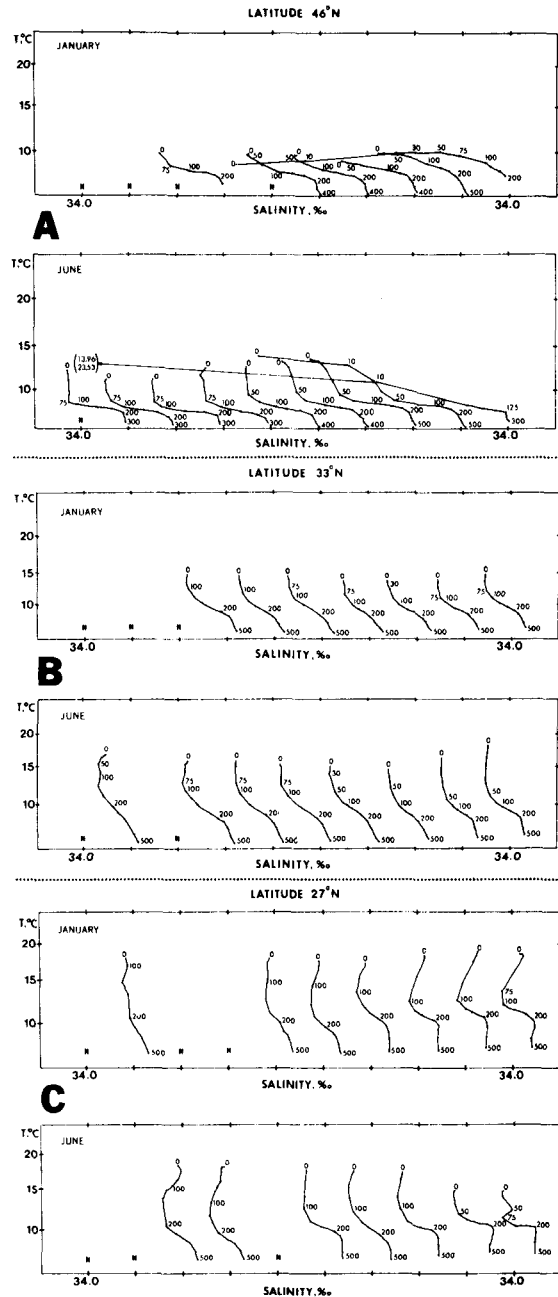

Figure 2. Mean temperature-salinity (T-S) curves for January and June for adjacent 1-degree squares from 10 degrees of longitude offshore to the coast at (A) 46°N; (B) 33°N; and (C) 27°N. In each diagram, the leftmost T-S curve corresponds to the 1-degree square located farthest offshore. The rightmost T-S curve corresponds to the 1-degree square closest to the coast. Each T-S curve is plotted relative to a salinity of 34⁰/oo at each tick mark, and tick marks are spaced at intervals of 1⁰/oo. The depth in meters of particular T-S pairs is identified on each curve. The letter N denotes that no data were available to compute a mean T-S curve at that location.

mation of a strong near-surface thermocline. The salinity profile is relatively constant, with a slight decrease with depth down to 50-75 m. The effects of coastal upwelling are evident in the T-S curves 3 to 4 degrees of longitude offshore, where there is relatively little seasonal change in the T-S structure between January and June. The cool water upwelled farther north at Point Conception during early summer is advected toward the south; seasonal warming is suppressed. The T-S curves farther offshore reveal the effects of lateral mixing (between the subarctic water mass flowing south and the subtropical water mass to the west) in the increased salinities (33.0-33.5⁰/oo) in the upper layers.

Farther south near Punta Eugenia (Figure 2C) the influence of an equatorial water mass is noted in the warmer, more saline (~34.5⁰/oo) water in the 200-500-m depth range in the first four 1-degree squares adjacent to the coast. This water mass indicates the poleward flow of Equatorial Pacific water beneath the equatorward surface flow of the California Current (Reid et al. 1958). This warm, saline countercurrent has been traced as far north as the coast of Washington (Cannon et al. 1975; Reed and Halpern 1976). The effects of coastal upwelling are again evident in the much colder surface waters during June at the two squares adjacent to the coast. Excluding these coastal squares during the months of maximum upwelling (upwelling-favorable winds occur during the entire year off Baja California, and maximum upwelling occurs in April and May; Bakun and Nelson 1977), the T-S structure in the upper 100 m is characterized by relatively constant salinity or a decrease in salinity with depth to a minimum value at 75-100 m, and is associated with a strongly stratified temperature profile. The well-defined January subsurface salinity minima in the three squares adjacent to the coast may result from anomalous northward surface flow, which transports southern, high-salinity water into the region.

These seasonal mean T-S curves (Figures 2A, B, and C) do not completely describe the total range of temperature-salinity structures along the entire coast and particularly not in the offshore squares, where some T-S curves are based on data from only three hydrographic stations. However, these data adequately represent the modification of the subarctic water mass in the trajectory of the California Current from north to south, and the mixing of the shallow salinity minimum—which is found at a depth of 50 m near its source region at 47°N (Reid 1973)—with higher salinity water to the west and below the minimum.

The T-S curves reveal that in the vicinity of the central and southern subpopulations of the northern anchovy (Figure 2B, C), vertical stability in the upper 100 m can be closely approximated by the vertical distribution of temperature (i.e., salinity is nearly constant with depth). However, north of about 40°N, vertical stability in the near-surface layers is strongly influenced by a large increase in salinity with depth. The influence of excess precipitation over evaporation and freshwater discharge from the Columbia River is evident in winter. More marked effects are apparent during summer (Figure 2A), when the plume structure contributes to strong thermal stratification in the upper 20-30 m of the water column within 300-500 km of the coast. In this case, upper-layer temperatures increase while salinity decreases; both effects contribute to less dense water at the surface and stronger vertical density gradients in the upper water column. Although an index of stability computed just from temperature data underestimates the correct magnitude, our analyses of the mean T-S relationships suggest that temperature data alone can also be used to compute qualitative indices of vertical stability in the principal spawning area for the northern subpopulation of the northern anchovy.

The index of vertical stability was computed from the file of MBT profiles archived in the Master Oceanographic Observation Data Set (MOODS) at the U.S. Navy's Fleet Numerical Oceanography Center (FNOC), Monterey, California. Our extract of this file contains a rather complete set of approximately 131,000 MBT casts taken in the California Current between 1931 and 1975. However, a substantial number of the profiles are serial or near-replicate casts taken at the locations of weather ships, coastal lightships, and U.S. Navy radar picket ships, which operated in the eastern North Pacific Ocean from 1960 to 1965. To eliminate some of this station-specific sampling bias, we subsampled the data set by removing profiles obtained within 56 km (30 n mi) and 24 h of each other. This editing reduced the extract file to approximately 74,000 profiles. Over 90 percent of these profiles extended to at least 137 m (450 ft). The reduced data set contains between two and three times the numbers of profiles as the NODC SDII file. In addition, the MBT data provide better vertical resolution for the stability calculations than can be achieved from the standard-depth hydrocast data.

Two parameters were computed for each MBT profile extending deeper than 50 m: (1) the mixed layer depth (MLD) and (2) the strength of the first significant stratification, which we have termed "thermocline strength." The majority of the MBT profiles were digitized at intervals of 5 m. Mixed layer depth was defined as the upper limit of the first 5-m interval in

which the temperature gradient ($\Delta T/\Delta Z$, Z positive downward) exceeded $-0.3°C$ per 5 m ($-0.06°C$ m^{-1}). The layer of first significant stratification was identified as the first depth interval below the mixed layer where the vertical temperature gradient exceeded $-0.06°C$ m^{-1}. The bottom of the thermocline was chosen to coincide with the upper depth of two successive 5-m intervals within which temperature gradients did not exceed $-0.06°C$ m^{-1}. The index of thermocline strength was then calculated as the temperature difference between the MLD temperature and the temperature at the bottom of the thermocline. The relationships among MLD, bottom of the thermocline, and thermocline strength are shown schematically in Figure 3, which also depicts summer and winter thermal structure typical of the eastern North Pacific Ocean (Tully 1964).

Thermocline strength and mixed layer depth were summarized by 1-degree square areas and long-term months and quarters within the same 1-degree latitude-longitude grid used to compile the mean distributions of wind speed cubed. Because the numbers of subsurface data are an order of magnitude less than the observations of surface wind, the mean distributions of the two stability indices are substantially "noisier" than the distributions of wind speed cubed, particularly in the offshore areas. Some of the sampling "noise" in the contoured fields has been removed by subjective smoothing. Within the region most intensively studied by the CalCOFI surveys during the last 30 years, the subsurface data are adequate to define coherent spatial patterns of the stability indices.

DISTRIBUTIONS OF WIND-MIXING AND STABILITY INDICES

The three indices that have been summarized are bulk estimates of the intensity of wind-generated turbulence production and the strength of upper-layer stratification. The thermal MLD approximates the depth to which turbulent processes (expressed as wind speed cubed) dominate. Thermocline strength measures the magnitude of the density gradient (vertical stability) beneath the mixed layer, that is, in the seasonal (summer) and permanent (winter) thermocline (Figure 3). A possible linkage between these environmental conditions and successful year classes of the northern anchovy has been related to the existence of chlorophyll maximum layers (Lasker 1975, 1978), which are found in the thermocline and in the upper nutricline. Chlorophyll maxima lie somewhat deeper off Washington and Oregon (Anderson 1972) than off southern California (Reid et al. 1978; Cullen 1981). Low mean turbulence production and relatively high
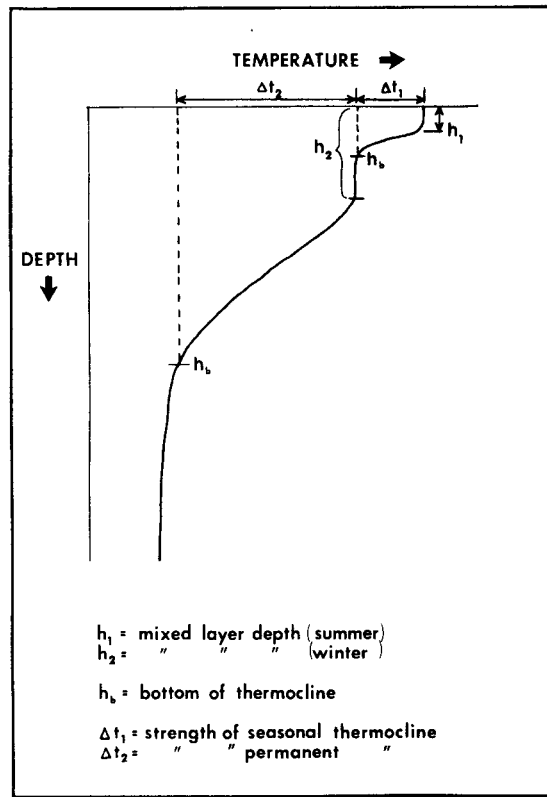

Figure 3. Schematic profile of temperature versus depth depicting typical summer and winter mixed layer and thermocline structure.

stability over a spawning season might favor persistent chlorophyll maxima; high turbulence production and low stability would not.

Spatial Patterns

Distributions of wind speed cubed, thermocline strength, and mixed layer depth for winter (December-February, Figure 4A) and summer (June-August, Figure 4B) illustrate characteristic features of the locations and peak spawning periods for the central and southern subpopulations (winter-spring spawners) of northern anchovy and for the northern subpopulation (summer spawners). During winter (Figure 4A) low turbulence production, moderate to strong upper-layer thermal stratification, and relatively shallow mixed layer depths characterize (1) the nearshore region (from the coast to 100 km offshore) in the Southern California Bight and (2) a broad area extending toward the southwest from southern Baja California. Both regions correspond to the general spawning areas for the central and southern stocks (Figure 1), although the spawning grounds for the southern stock have not been
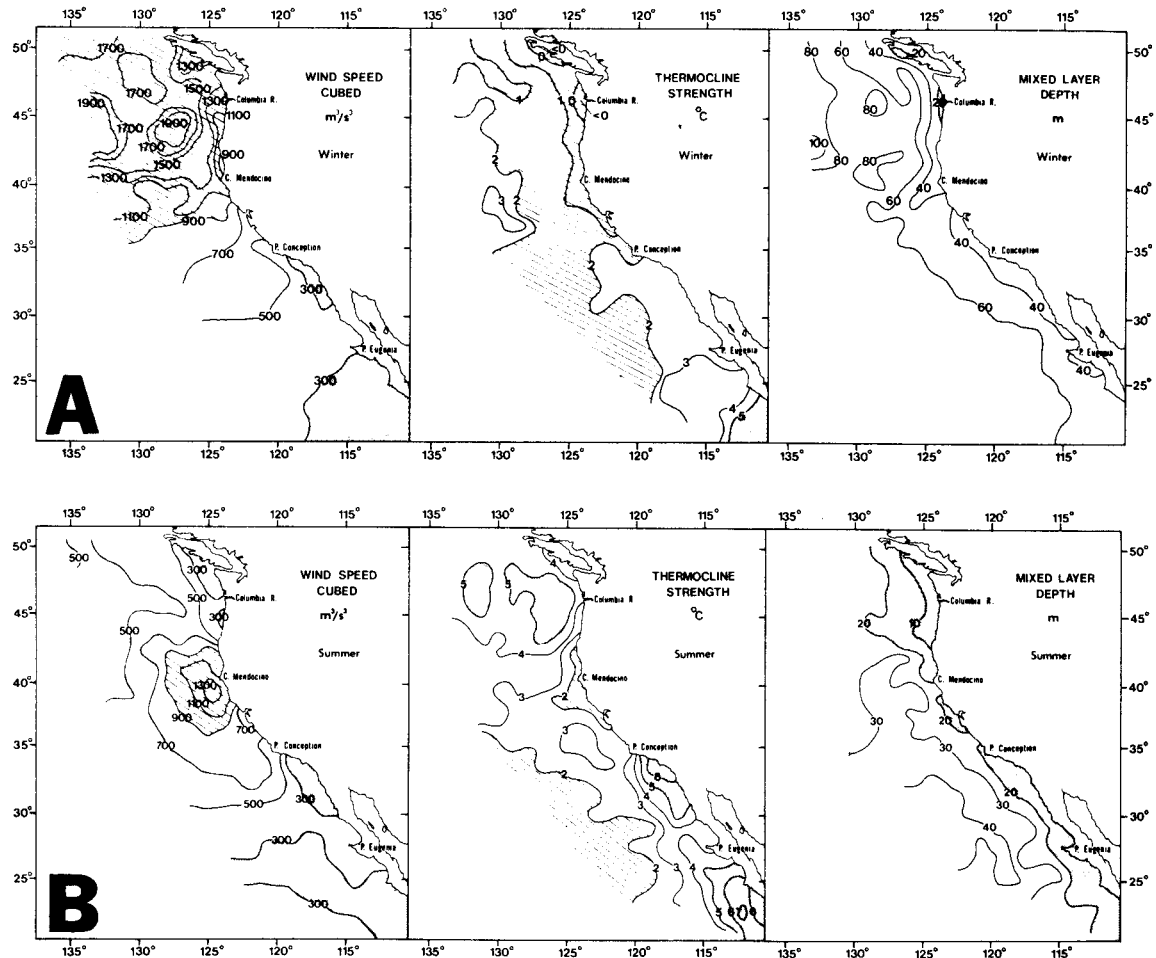
Figure 4. Mean distributions of wind speed cubed (m³s⁻³) indicating the rate of turbulent energy production, thermocline strength (°C), and mixed layer depth (m) for (A) winter (December-February) and (B) summer (June-August). Wind speed cubed is contoured at intervals of 200 m³s⁻³. Values less than 300 m³s⁻³ are shaded, and values greater than 900 m³s⁻³ are hatched. Thermocline strength is contoured at intervals of 1°C. Shaded areas are greater than 5°C; hatched areas denote a thermocline strength less than 2°C. Mixed layer depth is contoured every 20 m, and values less than 20 m are shaded.

completely described. Lower values of wind speed cubed (<200 m³s⁻³), stronger stratification, and shallower mixed layers (~30 m) occur close to the coast. The local spatial minimum in wind-generated turbulence in the Southern California Bight persists throughout the year and is consistent with a decrease in the magnitude of the equatorward surface wind in the lee of Point Conception. A nearshore maximum in wind speed cubed just south of Punta Baja (near 30°N values approach 500 m³s⁻³) corresponds to a permanent region of negative wind stress curl that reaches the coast in the vicinity of Punta Eugenia (Nelson 1977). High turbulence production, weak stratification, and deep mixed layers characterize the entire

region north of San Francisco, with the exception of a small area off the mouth of the Columbia River, for which mixed layer structure is not completely defined by temperature alone (see Figure 2A).

The similarities among the distributions of wind speed cubed and the two indices of upper-layer stratification are obvious in summer (Figure 4B). South of Point Conception, the two regions of low turbulence production are associated with shallow mixed layers (~20 m) and the highest values of thermocline strength. These features (i.e., high stability in combination with low turbulence) are not particularly well related to the central stock's spawning cycle, which passes through a minimum between July and

119

October (Smith and Richardson 1977). This simply indicates that factors other than the simultaneous occurrence of low turbulence and high stability influence the timing of peak spawning. The highest values of wind speed cubed occur in the region of maximum upwelling off Cape Mendocino, which is also characterized by the weakest stratification. Off the Columbia River there is a strong correspondence between the patterns of wind speed cubed, thermocline strength, and mixed layer depth and Richardson's (1980) distributions of eggs and larvae of the northern subpopulation of *E. mordax*. The strong influence of the Columbia River plume is apparent in the high values of thermocline strength and the shallowest thermal MLD's in the entire California Current region. It is possible that, because of this strong upper-layer stratification, higher values of turbulence production may be associated with spawning success for the northern subpopulation in summer (e.g., the area within the 500 m^3s^{-3} contour off Vancouver Island, Washington, and Oregon, Figure 4B) than for the central and southern subpopulations in winter (Figure 4A).

Seasonal Variability

Annual cycles of wind speed cubed (Figure 5A, B) and thermocline strength (Figure 5C) are shown for selected 1-degree squares near the principal spawning grounds for the three subpopulations of the northern anchovy. A strong correspondence between the timing of peak spawning and the magnitude of the mean wind-generated turbulence can be demonstrated for each of the three regions. However, the relationship of the spawning cycle to the annual cycle of vertical stability (thermocline strength) shows less consistency between regions.

The southern stock spawns off southern Baja California (25-28°N) during winter and spring; peak larval abundance occurs from January to March (Smith 1972). Wind speed cubed fluctuates about a nominal value of 300 m^3s^{-3} from September to February (curve 1, Figure 5A); mean values exceed 400 m^3s^{-3} after the onset of upwelling-favorable winds in March and April (Bakun and Nelson 1977). During this period, thermocline strength decreases from a maximum (>6°C) in October to a minimum (~0-1°C) in January (curve 1, Figure 5C).

The central stock spawns in the Southern California Bight (30-34°N) throughout the year, with a maximum from February to April (Smith and Richardson 1977). The Southern California Bight is characterized by uniformly low turbulence production throughout the year (curve 2, Figure 5A). At this location, the small peak in the annual cycle (~300 m^3s^{-3}) occurs during

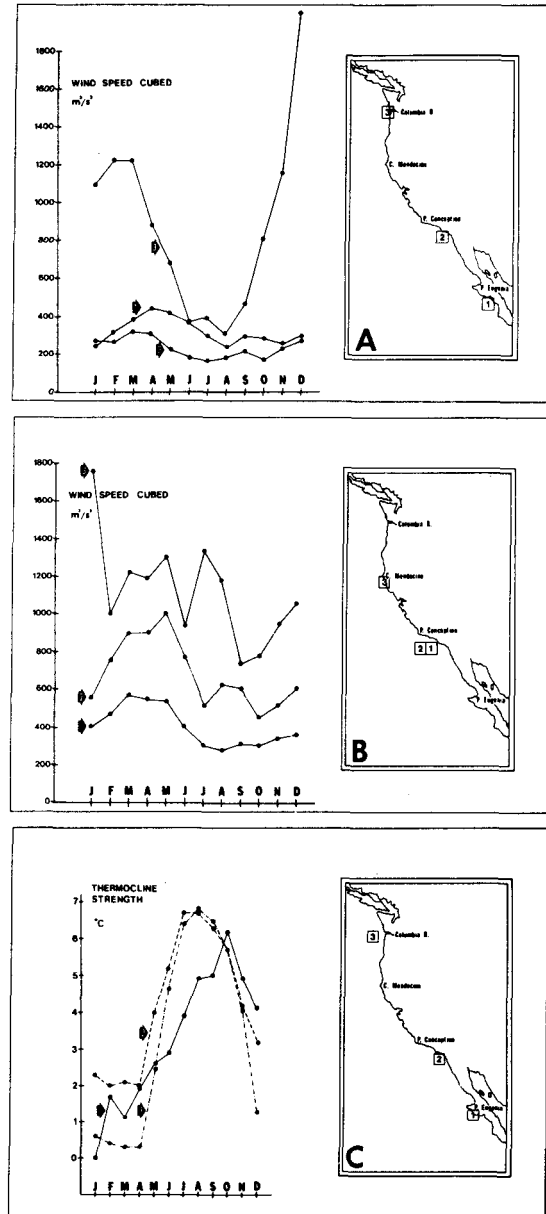Figure 5. Annual cycles of wind speed cubed (m^3s^{-3}) and thermocline strength (°C) at selected 1-degree squares along the coast. Characteristic values of wind speed cubed and thermocline strength in the three northern anchovy spawning areas are shown in panels A and C. Mean values of wind speed cubed typical of the offshore regions of the Southern California Bight and the region of maximum upwelling off Cape Mendocino are displayed in panel B.

the peak spawning season; thermocline strength is nearly constant, but at a minimum (~2°C), from January to April (curve 2, Figure 5C). The seasonal

transition to a shallow mixed layer structure (i.e., strong upper-layer stratification) occurs between April and May, but the precise timing of the transition period cannot be resolved by these long-term mean data. According to Richardson (1980), the northern stock spawns in the Columbia River plume (44-46°N) from June to August; spawning is concentrated in July. Off the mouth of the Columbia River, upper-layer stratification increases to a maximum (6-7°C) from July to September (curve 3, Figure 5C). It is also notable that mean wind speed cubed decreases to a minimum (350-400 m^3s^{-3}) through the spawning season (curve 3, Figure 5A).

Taken in isolation, these data suggest a relationship between peak spawning periods and optimum levels (not necessarily minimum levels) of wind-generated turbulent mixing. We note that the cube roots of the mean values associated with the spawning seasons (200-400 m^3s^{-3}) lie close to an apparent low wind-speed threshold for the formation of oceanic whitecaps (Monahan 1971), a more obvious, visual index of wind-generated turbulence production. In this context, the proper relationship between the mean wind speed cubed and the mode of the wind-speed probability distribution (which typically shows Poisson rather than Gaussian behavior) is important. From an examination of selected frequency distributions presented by Nelson (1977), we concluded that mean values of 200-400 m^3s^{-3} are entirely consistent with modal wind speeds in the range 3-5 m s^{-1}. This range of values is just below the threshold wind speed ($\sim$5 m s^{-1}) that Therriault and Platt (1981) used to distinguish biological (low turbulence) from physical (high turbulence) control of phytoplankton patchiness.

The data plotted in Figure 5B demonstrate a large offshore increase in turbulence production in the Southern California Bight (curves 1 and 2) and illustrate the seasonal progression of wind speed cubed that characterizes the region of maximum upwelling (curve 3). The zonal section represented by curve 2 (Figure 5A) and curves 1 and 2 (Figure 5B) shows a monotonic increase in wind speed cubed from values less than 300 m^3s^{-3} near the coast to values exceeding 900 m^3s^{-3} offshore. The amplitude of the annual cycle is substantially larger at the offshore locations as well. Off Cape Mendocino, wind-generated turbulence production is high throughout the year; highest values are associated with winter storms and strong equatorward surface winds during summer.

Seasonal isogram plots of wind speed cubed and thermocline strength (Figure 6A) and two independent estimates of mixed layer depth (Figure 6B) were constructed from the long-term monthly mean values within 3 degrees of the coast. Wind speed cubed was

plotted for the 1-degree squares immediately adjacent to the coast. The stability indices were averaged over three 2-degree squares at each latitude to increase the number of observations per averaged value.

The seasonal cycles of wind speed cubed and thermocline strength (Figure 6A) show strong similarities among the timing and locations of regions characterized by low wind-induced turbulence (<300 m^3s^{-3}) and strong vertical stability (thermocline strength >5°C). The relative minima (wind speed cubed) and maxima (thermocline strength) in the time-space domain nearly coincide with the known spawning periods and spawning grounds for the northern anchovy. The notable exception occurs between 30°N and 35°N in the Southern California Bight.

The coastal region between 43°N and 48°N is characterized by low turbulence and strong upper-layer stratification from June to September. During this same period, the thermal MLD's are less than 20 m over the entire region north of 40°N (Figure 6B). Minimum MLD's occur in May and June in response to peak freshwater discharge from the Columbia River. Between Cape Mendocino (40°N) and Point Conception (35°N) high values of wind speed cubed, low stability, and shallow mixed layers are associated with strong coastal upwelling during spring and summer. During winter, frequent and severe storms cross this region (north of 40°N), drive the mixed layer deeper (Figure 6B), and decrease upper-layer stratification to a minimum (Figure 6A).

Because of the strong influence of the Columbia River plume on vertical stability, we checked the consistency of the thermal mixed layer depths (based on MBT data) by constructing a seasonal isogram plot of pycnocline depth. Pycnocline depth was defined as the upper depth of the interval for which stability (defined by Equation 1) was a maximum, and mean values were computed from the hydrographic data in the NODC SDII file. Comparison of the two panels in Figure 6B shows close agreement between thermal MLD and pycnocline depth along the entire coast during the summer. A weaker relationship is evident during winter, although the two methods show similar seasonal trends.

The nearshore region in the Southern California Bight (30-35°N) is characterized by uniformly low values of wind speed cubed (<300 m^3s^{-3}) throughout the year, with the exception of a local maximum at 33°N from February to April (Figure 6A). Upper-layer stratification follows a well-defined, large-amplitude annual cycle. There is a lack of agreement between the peak spawning period for the central subpopulation of E. mordax (January-April) and maximum thermocline strength (July-September). Thus the simultaneous oc-
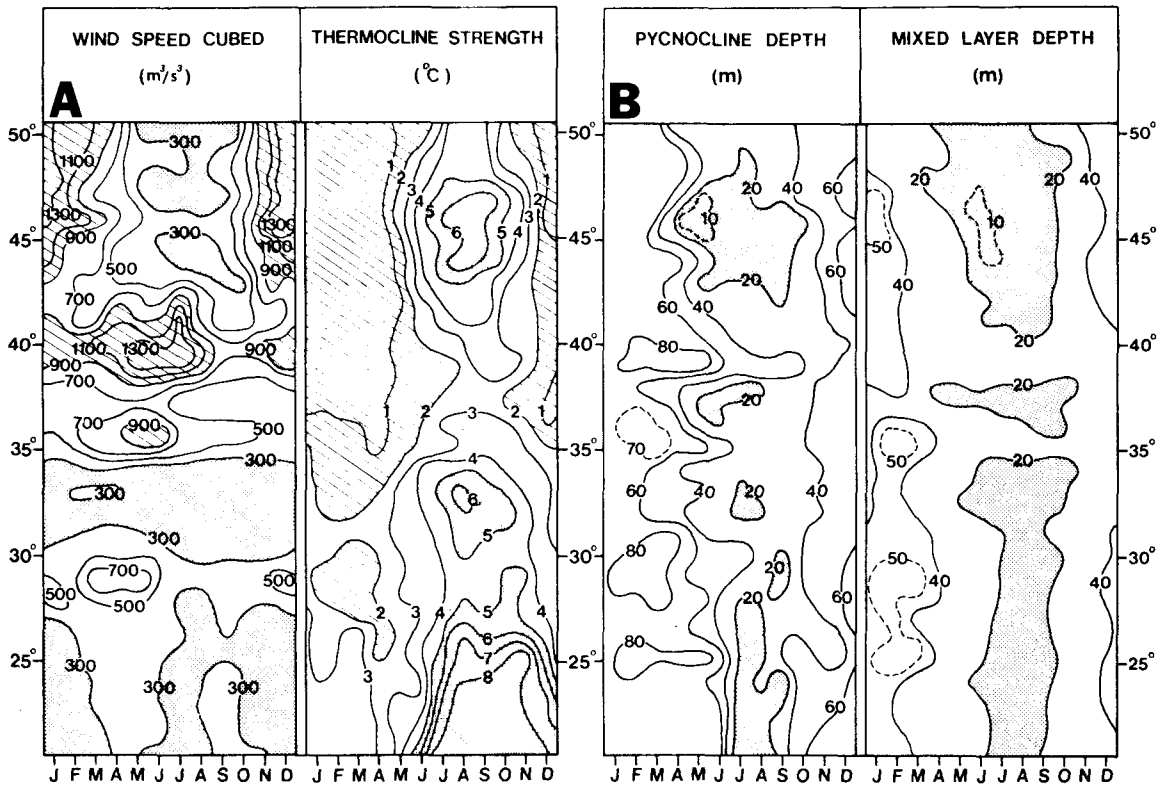
Figure 6. Seasonal cycles of (A) wind speed cubed (m³s⁻³) and thermocline strength (°C) and (B) pycnocline depth (m) and mixed layer depth (m) near the coast. Means of wind speed cubed were computed by month for 1-degree squares immediately adjacent to the coast. Monthly means for thermocline strength, pycnocline depth, and mixed layer depth are averages of the values within 3 degrees of the coast at each latitude. In panel A, wind speed cubed is contoured at intervals of 200 m³s⁻³. Values less than 300 m³s⁻³ are shaded, and hatched areas correspond to mean values greater than 900 m³s⁻³. Thermocline strength is contoured every 1°C. Shaded areas are greater than 5°C; hatched areas are less than 2°C. In panel B, pycnocline depth and mixed layer depth are contoured every 20 m. Layer depths less than 20 m are shaded.

currence of high stability and low turbulence may not be necessary for spawning success. This also suggests that high stability (and shallow mixed layers) prior to or during the peak spawning months may also contribute to adverse spawning conditions, for example, by inhibiting the upward flux of nutrients into the mixed layer and thereby decreasing primary production.

South of 30°N, a pattern of low turbulence production is broken twice over the annual cycle: (1) from March to June in conjunction with strong, upwelling-favorable surface winds, and (2) during the fall when tropical storms occasionally impinge on Baja California. This region is also characterized by relatively strong thermal stratification (values exceed 3°C; maximum stability occurs from August to November, Figure 6A) and shallow mixed layers (20-40 m) throughout the year. If upper-layer stability and wind-generated turbulent mixing were the only two factors associated with the "critical period" for larval anchovies, then the extended period of low turbulence

and relatively high stability near the coast and south of 27°N suggests that spawning conditions might be more favorable for the southern subpopulation than for the central stock. Of course, other factors, such as the spatial structures of predator-prey populations (Smith and Lasker 1978), may interact with the processes addressed in this paper to regulate spawning success, particularly in regions of low mean values of wind speed cubed (e.g., in the Southern California Bight).

Turbulence, Transport, and Stability on the Principal Spawning Grounds

The long-term mean distributions mapped in Figures 4-6 corroborate Lasker's (1975, 1978) explanation of the "critical period" concept (i.e., a stable ocean in the absence of turbulent mixing is a prerequisite for larval survival). The spawning grounds for each of the three subpopulations of the northern anchovy are characterized by low values of wind speed cubed during the peak spawning seasons; mod-
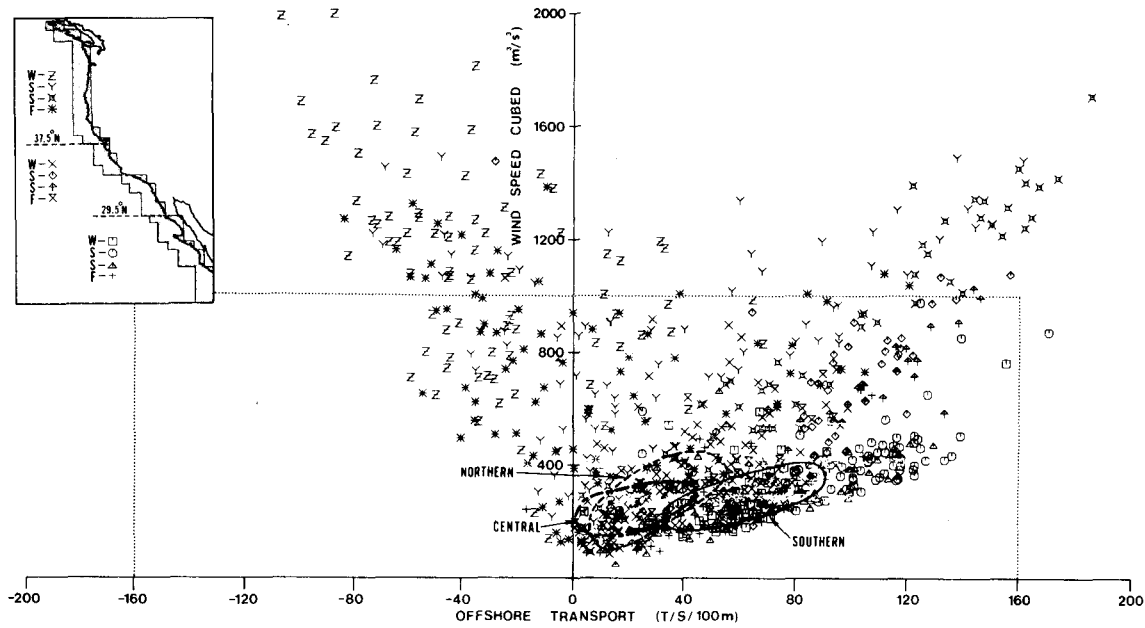
Figure 7. Scatter diagram of wind speed cubed (m^3s^{-3}) versus offshore Ekman transport ($t\ s^{-1}$ per 100 m). Mean monthly values are plotted for each 1-degree square within the shaded region shown in the inset. Negative values denote onshore transport. Symbols are coded according to season (W,S,S,F) within each of the three coastal regions shown in the inset. Winter corresponds to December-February. Values of wind speed cubed and offshore transport associated with the peak spawning months and spawning grounds for the southern, central, and northern subpopulations of E. mordax are enclosed by solid, dashed, and dotted lines, respectively. The dotted lines at 1000 m^3s^{-3} and ± 160 $t\ s^{-1}$ per 100 m correspond to the limits of the expanded scatter diagrams in Figure 8.

erate to strong upper-layer stratification is associated with two of the three spawning seasons and locations. During the peak spawning season for each subpopulation, low values of wind speed cubed correspond to equatorward surface wind stress (Nelson 1977), implying some degree of offshore transport in the surface layers and upwelling near the coast. Surface transport has been discussed (Parrish et al. 1981) as an alternate but not mutually exclusive "critical period" hypothesis. Therefore, an index of offshore Ekman transport was used as an additional variable to characterize the wind field over the principal spawning grounds.

Scatter diagrams of turbulence versus transport were constructed by plotting the long-term monthly mean values of wind speed cubed against estimates of offshore Ekman transport (Figures 7 and 8). Nelson's (1977) surface wind-stress values were used to compute the offshore directed component of surface Ekman transport (using the method described by Bakun and Nelson, 1977) for each 1-degree square area within a region extending from the coast to 2 degrees of longitude offshore. The total ensemble of approximately 720 possible monthly mean pairs of wind speed cubed and offshore transport was partitioned into three geographic regions with breaks at 29.5°N and 37.5°N (approximate stock boundaries)

and into four quarters, with winter defined as December-February. Twelve different symbols were used to distinguish the spawning seasons and spawning grounds. The total data set was subsampled and replotted in four additional scatter diagrams to illustrate the salient points more clearly (Figure 8). Different letter symbols are shown in Figure 8, analogous procedures were used to construct the diagrams. Each of the points plotted in these diagrams corresponds to a pair of long-term monthly means. Sampling variability produces large scatter about the means. Thus, these diagrams do not represent all possible combinations of turbulence and transport and should be considered as mean "envelopes" characterizing the average environmental conditions in the region.

Low turbulence and weak offshore transport are common to all three spawning regions (Figure 7), which occupy overlapping positions near the origin in the diagram. Four distinct regimes are evident in this diagram: (1) the entire left portion (i.e., onshore transport) is characteristic of fall-spring off the Pacific Northwest; (2) the high wind speed cubed/high offshore transport region (i.e., greater than 600 m^3s^{-3} and 80 $t\ s^{-1}$ per 100 m) distinguishes the region of maximum upwelling from Point Conception (35°N) to Cape Blanco (43°N) in spring and summer; (3) the
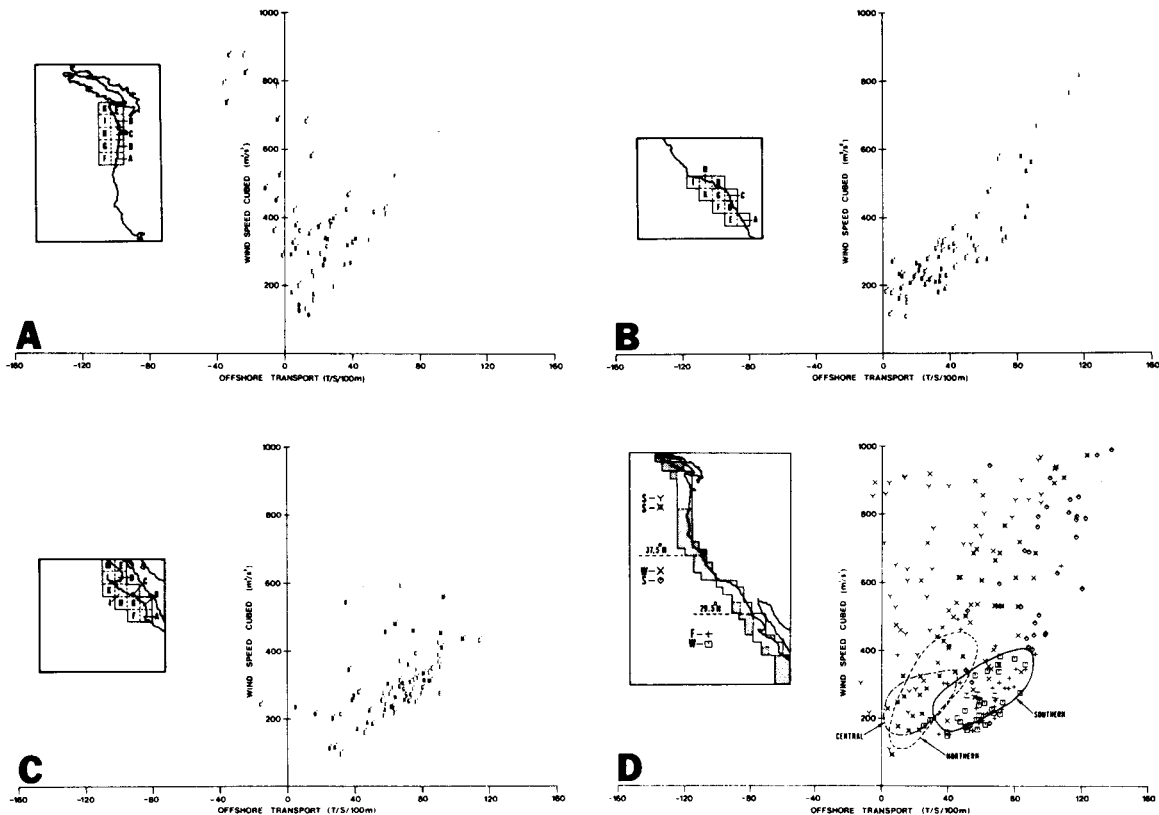
123

Figure 8. Scatter diagrams of wind speed cubed (m^3s^{-3}) versus offshore Ekman transport (t s^{-1} per 100 m) in the (A) northern, (B) central, and (C) southern spawning regions. Values for the nonspawning areas are plotted in panel D. Mean monthly values are plotted for March-August in panel A; December-May in panel B; and September-February in panel C. Negative values denote onshore transport. Symbols are coded according to the location of the 1-degree squares shown in the insets, and primed letters correspond to the first three months of the six months plotted in each of panels A, B, and C. Values plotted in panel D correspond to the shaded regions outside the principal spawning areas (inset), but during the peak spawning seasons in each of the three regions. The symbols are coded according to season (W,S,S,F) and region, and the enclosed portions of the scatter diagram labeled northern, central, and southern are the same as those shown in Figure 7. Note the change of scale for wind speed cubed in this figure compared to Figure 7.

low-turbulence/high transport area is associated with the Baja California upwelling system in the spring; and (4) the low wind speed cubed/weak offshore transport region (i.e., less than 400 m^3s^{-3} and 80 t s^{-1} per 100 m) almost exclusively encompasses data from the principal spawning regions during the peak spawning seasons. The overlap among the three spawning regions would have been more pronounced if we had plotted wind speed cubed against the alongshore component of surface stress (thereby removing the effect of latitudinal variation in the Coriolis parameter; offshore transport is inversely proportional to the Coriolis parameter f, where f = 0.0001458 SIN $\emptyset$ s^{-1} and $\emptyset$ is the geographic latitude).

Separate scatter diagrams were constructed for each of the three principal spawning regions but only for the 6 months spanning the spawning season in each region

(Figure 8A, B, and C). Data for the nonspawning regions during the same 6-month periods are plotted in Figure 8D to identify other coastal locations characterized by low turbulence and weak offshore transport. Our interpretation of these scatter diagrams follows the main conclusion drawn from the spatial and temporal distributions: the months and locations associated with low wind-generated turbulence (and weak offshore transport) are also the principal spawning seasons and spawning grounds for each of the three subpopulations of the northern anchovy.The lowest values of wind speed cubed and offshore transport correspond to the squares immediately adjacent to the coast (e.g., symbols A, B, C, D, and H in Figure 8B). Examination of anchovy larvae distributions for 1966-1979 (Hewitt 1980) suggests a tendency for higher larval abundance within 100 km of the coast

than offshore, which would be consistent with greater spawning success in the nearshore, low-turbulence regions.

There are a few locations and months for which the mean wind speed cubed/offshore transport pairs fall within the areas on the diagrams occupied by the spawning stocks (Figure 8D). For the southern stock, most of these data are from 1-degree squares located well offshore (e.g., the entire shaded block south of Cabo San Lucas at 25°N). Virtually no other locations between 29.5°N and 37.5°N can be characterized by the low-turbulence/weak transport values associated with the central stock's spawning grounds. The additional data coinciding with the position occupied by the northern stock come from the 1-degree squares adjacent to Vancouver Island and from the nearshore region in the vicinity of San Francisco. Recent data suggest that the coastal waters adjacent to San Francisco Bay provide a suitable habitat for winter-spring spawning of *E. mordax* (Stepanenko 1981[1]).

Analogous procedures were used to construct a scatter diagram of wind speed cubed versus thermocline strength (Figure 9). For this diagram, quarterly mean values of wind speed cubed and thermocline strength were used. Thus the numbers of wind speed cubed/thermocline strength data pairs have been reduced by a factor of three relative to the data points plotted in Figure 7. Although this particular diagram shows a great deal of scatter, there is evidence for an inverse relationship between wind speed cubed (turbulence) and thermocline strength (stability). High turbulence (large wind speed cubed) and weak stability (low thermocline strength) correspond to winter storm activity and deep mixed layers off the Pacific Northwest, although similar turbulence/stability conditions occur off Cape Mendocino during spring and summer. High stability and relatively low values of wind speed cubed characterize Baja California in the fall (symbol D, Figure 9). The majority of the months and locations associated with the peak spawning seasons on each of the spawning grounds (symbols A, B for the southern stock; E, F for the central stock; L for the northern stock) lie within a relatively narrow range of values for wind speed cubed (200-400 m^{3}s^{-3}) and thermocline strength (2-5°C). This is evident in the close agreement among the three envelopes enclosing these points for each stock. For similar values of wind speed cubed in each region, stability (thermocline strength) is slightly higher on the spawning grounds for the southern and northern stocks of *E. mordax* than for the central stock.

[1]Stepanenko, M.A. Assessment of stocks and reproduction conditions of some commercial fish off the Pacific coast of the North America in 1980. Mimeograph report, Pacific Research Institute of Fisheries Oceanography (TINRO), Vladivostok, 1981, 21 p.
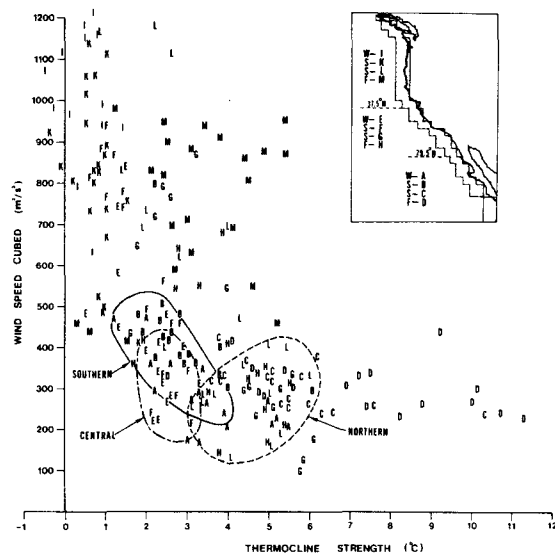

Figure 9. Scatter diagram of wind speed cubed (m^{3}s^{-3}) versus thermocline strength (°C). Mean quarterly values are plotted for each 1-degree square within the shaded region shown in the inset. Symbols are coded according to season (W,S,S,F) within each of the three coastal regions. Winter corresponds to December-February. Values of wind speed cubed and thermocline strength associated with the peak spawning months and spawning grounds for the southern, central, and northern subpopulations of *E. mordax* are enclosed by solid, dashed, and dotted lines, respectively.

DISCUSSION

Historical surface wind observations and subsurface temperature data from the California Current region have been used to compile long-term monthly mean distributions of two indices related to (1) the rate of turbulent energy production by the wind (wind speed cubed), and (2) the vertical stability of the upper water column (thermocline strength). Characteristic spatial patterns (Figure 4) and annual cycles (Figures 5 and 6) of these indices were discussed in relation to the principal spawning grounds and peak spawning seasons of the three subpopulations of the northern anchovy, *Engraulis mordax*. A strong correspondence was shown among the locations and seasons characterized by low wind speed cubed (turbulent mixing) and the timing of the spawning cycle for each stock. A weaker correspondence of the spawning cycle to relatively high thermocline strength (vertical stability) was demonstrated. Each of the spawning regions in the California Current is also associated with weak coastal upwelling and offshore transport during the respective spawning season (Figures 7 and 8). Bakun and Parrish (1982) show similar relationships among the regions of low turbulence production and the principal spawning grounds of the Peruvian anchoveta, *Engraulis ringens*.

One interpretation of these long-term mean data is

125

that reproductive strategies have evolved in response to "optimum" levels of turbulent mixing in the stable layers of the upper ocean, rather than to minimum levels of turbulence (or to maximum vertical stability). There are two important aspects to this rationale. In the complete absence of wind stirring or (upwelling), nutrient fluxes into the mixed layer would be substantially reduced, and phytoplankton production would decrease. Therefore, some degree of mixing and entrainment of nutrients at the base of the mixed layer would be required to maintain adequate concentrations of food for first-feeding larval anchovies. On the other hand, if the "optimum" level of turbulent mixing was frequently exceeded by large amounts, then destruction of fine-scale food strata and dispersion of larval anchovies could lead to recruitment failure, particularly if unfavorable conditions persisted through the spawning season (Lasker 1978). A similar argument can be made that too much stability prior to or during a spawning season might produce equally adverse spawning conditions by severely inhibiting the upward flux of nutrients and reducing primary production. There is evidence to suggest that the long-term monthly mean values of wind speed cubed that characterize the spawning grounds of the three subpopulations of *E. mordax* are consistent with a "threshold" wind speed ($\sim$5 m s^{-1}) associated by Kullenberg (1978) and Therriault and Platt (1981) with horizontal patchiness in phytoplankton distributions.

Mean distributions of environmental indices, which represent highly nonlinear, time-dependent physical processes (e.g., wind speed cubed), are meaningful to investigations of recruitment variability if, for example, pattern recognition can be used to identify normal requirements for reproductive success. In this context, the spatial patterns and annual cycles of wind speed cubed and thermocline strength discussed in this paper are useful, and corroborate Lasker's experimental evidence (1975, 1978). However, to determine the degree to which turbulence and stability have exerted a limiting control on spawning success of the northern anchovy over the past 14 years, reasonably complete time series data, on space and time scales appropriate to the biological processes, are required. Because the linkage between the physical processes (wind speed cubed) and recruitment success (year-class strength) is by no means direct, it is not reasonable to expect "any single mechanism to explain larval survival in all cases" (May 1974).

A 14-year time series (1968-81) of daily mean wind speed cubed indices (Figure 10) was constructed for a representative location in the Southern California Bight (33°N, 119°W). An estimate of the surface wind

was computed from the 6-hourly northern hemisphere surface pressure analyses available at Fleet Numerical Oceanography Center, using the method described by Bakun (1973). The daily values displayed in Figure 10 are means of the cube of the wind speed for the four synoptic samples per day. These time series data are characteristic of physical processes integrated over spatial scales (typically 3-degree resolution) which are 1 to 2 orders of magnitude larger than the horizontal scales associated with plankton patchiness and larval feeding. The indices are also uncalibrated in terms of absolute magnitude (Bakun 1973). Nevertheless, we feel that the analyzed meteorological fields offer a means of reconstructing consistent time-histories of the physical processes (e.g., wind speed cubed, offshore transport) that may have limited recruitment, thus causing the wide variations in year-class size over the past 14 years of the anchovy fishery. A similar time series of the stability indices could not be assembled because appropriate subsurface data do not exist.

The striking features of the daily wind speed cubed series are the large pulses over relatively restricted time periods during the spawning season (December-April). The characteristics distinguishing the spawning season of one year from that of another seem related to the frequency of occurrence of wind speed cubed "events" above a threshold value. In terms of Lasker's first-feeding hypothesis, favorable spawning seasons leading to strong year classes (e.g., 1976, 1978) contain relatively fewer events of magnitude exceeding a critical value, whereas spawning seasons resulting in poor year classes (e.g., 1975, 1977) are characterized by relatively more frequent, extended periods of intense wind events. Indeed, the first-feeding hypothesis has been largely formulated on the basis of field observations obtained before and after a period of strong winds during 1975 (Lasker 1975, 1978) and during the drought year spanning the 1975-76 spawning season (Lasker 1981b). Interestingly enough, the period of strong winds in February 1975 (also a period of strong upwelling) was followed by an even more intense mixing event (also strong upwelling) near the end of March—the largest such event during the spawning season over the 14-year record. It is likely that the occurrence of both of these events within one month contributed to the highest estimated recruitment failure in the history of the anchovy fishery (Smith et al. 1981).

One simple way of reducing the daily time series data to a quantitative index relating to the history of the fishery is to integrate the wind speed cubed index over the spawning season (i.e., form the December-February mean). These values (or the means for several different combinations of months from December
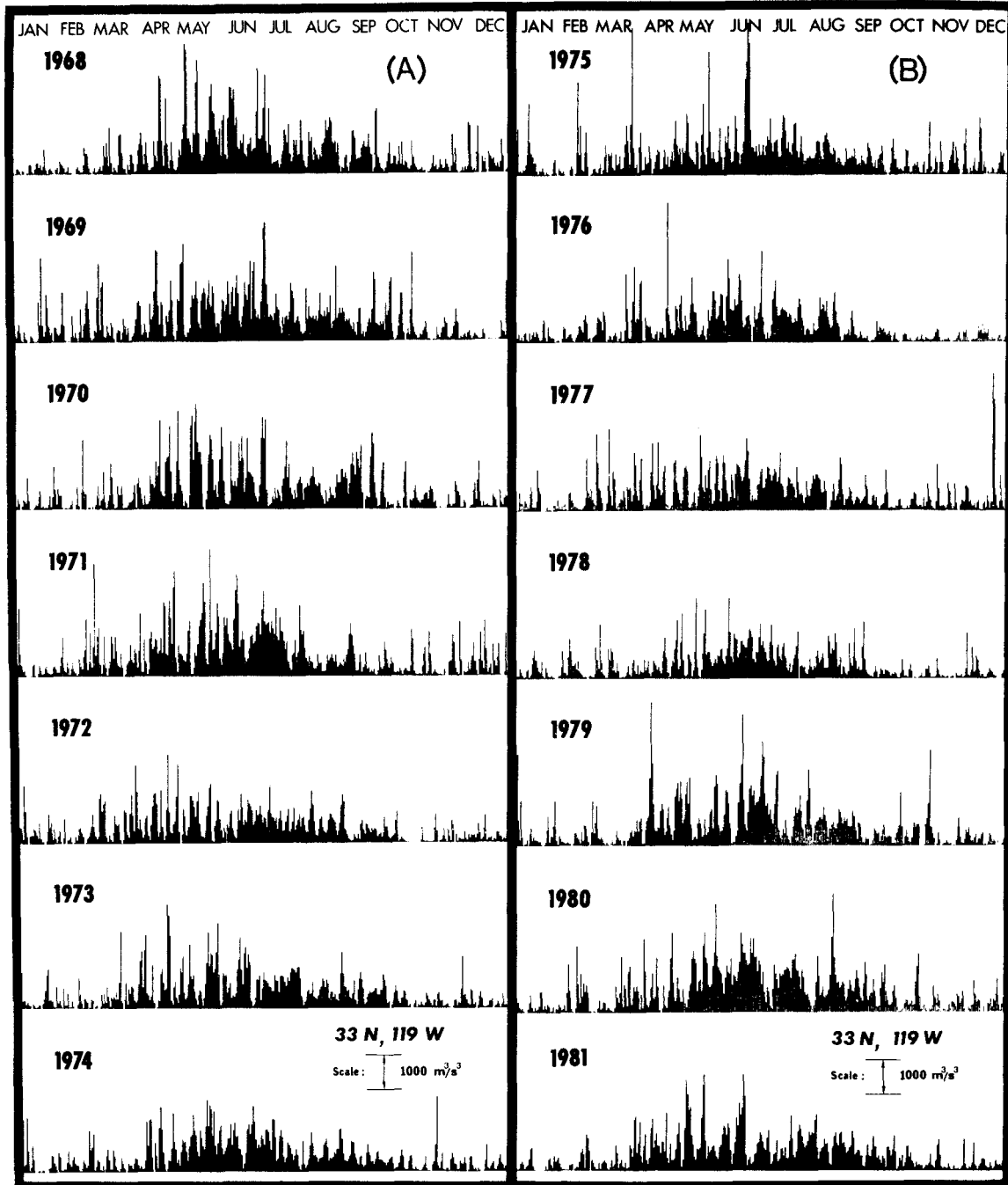
126

Figure 10. Daily indices of wind speed cubed (m^3s^{-3}) at 33°N, 119°W for *(A)* 1968-74, and *(B)* 1975-81. Daily values were derived from 6-hourly surface atmospheric pressure analyses. Values are scaled according to the key on each plot.

to April) could be used to test the relationship of wind-induced turbulence to recruitment and year-class strength, for example, by regressing the values of the intensity of wind speed cubed, averaged over the spawning season, against estimates of year-class size (Mais 1981) or by using rank correlation methods to compare the relative ranks of wind speed cubed with relative ranks of spawning success (Smith et al. 1981). Such statistical tests are beyond the scope of this paper. However, it is unlikely that the variability in year-class strength would be well described by a linear correlation with bulk estimates of a highly non-linear process, particularly considering the limited degrees of freedom in the data.

This is not to imply that turbulence and stability may not exert a control on spawning success (i.e., the lack of a significant statistical relationship would not be sufficient to reject the wind-turbulence hypothesis), but rather to suggest that the mean intensity of wind speed cubed over the spawning season may not provide a useful way to quantify the integrated effects of physical processes on time scales critical to larval first feeding. A simple calculation demonstrates our point. A sequence of 30 days in which the (uncalibrated) daily wind speed cubed averages 300 m^3s^{-3} would have exactly the same monthly mean as a sequence of 30 days in which periods of 4 days with daily means of 125 m^3s^{-3} are followed by an event of magnitude 1000 m^3s^{-3}. In the first situation, mixing and stability conditions would most likely favor the formation of chlorophyll maximum layers, leading to recruitment success. In the second case, recruitment failure would result from episodic destruction of stratified layers during the critical period (2-3 days) after yolk-sac absorption (Lasker et al. 1970).

It is likely that the most favorable conditions for larval survival correspond to extended periods of low-turbulence "windows" prior to and continuing through the critical period. In terms of this requirement, at least five important features in the wind speed cubed time series need to be quantified in relation to the "critical period" requirements of larval anchovy: (1) the required length of the low-turbulence "windows," (2) the magnitude and duration of events exceeding the low-turbulence threshold, (3) the frequency with which high-turbulence events recur, (4) the association of high-turbulence events with coastal upwelling or downwelling processes, and, perhaps most important, (5) the timing of the spawning cycle in relation to the sequence of turbulence events. A proper analysis of the last feature would require detailed information on the birthdate distributions of surviving anchovy (Methot 1981).

We suggest two methods that might be used to further investigate the effects of physical mechanisms on reproductive success. A statistical approach could be used to search through a time series of daily (or 6-hourly) values of wind speed cubed, to find the combinations of low-turbulence "windows" and high-turbulence "events" that best characterize a spawning season as favorable or unfavorable in terms of the stability requirements of Lasker's first-feeding hypothesis. Examination of these data in relation to data on intensity of spawning, birthdate distributions (Methot 1981), and year-class survival (Mais 1981; Smith et al. 1981) might suitably test the wind turbulence hypothesis.

An alternate method would be to investigate the evolution (generation, maintenance, and destruction) of fine-scale food strata in the upper layers of the ocean by coupling existing state-of-the-art one-dimensional mixed layer models (e.g., Garwood 1977) with appropriate biological models (Steele 1977) to test the sensitivity (biological response) to different characterizations of atmospheric forcing and to different initial conditions. Substantial new field measurements of both physical and biological processes over an extended period of the spawning season would be required to initialize and verify the model predictions. A carefully designed physical/biological mixed layer model would complement existing laboratory and field programs, and offers a method to properly integrate the effects of wind-generated turbulence over a spawning season, thereby contributing to our understanding of the important linkages of physical processes to recruitment success of the northern anchovy.

ACKNOWLEDGMENTS

LITERATURE CITED

Anderson, G.C. 1972. Aspects of marine phytoplankton studies near the Columbia River, with special reference to a subsurface chlorophyll maximum. In A.T. Pruter and D.L. Alverson (eds.), The Columbia River estuary and adjacent ocean waters. Univ. Wash. Press, Seattle and London, p. 219-240.

Bakun, A. 1973. Coastal upwelling indices, west coast of North America, 1946-71. U.S. Dep. Commer., NOAA Tech. Rep. NMFS SSRF-671, 103 p.

Bakun, A., and C.S. Nelson. 1977. Climatology of upwelling related processes off Baja California. Calif. Coop. Oceanic Fish. Invest. Rep. 19:107-127.

Bakun, A., and R.H. Parrish. 1980. Environmental inputs to fishery population models for eastern boundary current regions. *In* G.D. Sharp (ed.), Workshop on the effects of environmental variation on the survival of larval pelagic fishes, Lima, Peru, 20 April-5 May 1980. IOC Workshop Rep. 28, UNESCO, Paris, p. 67–104.

———. 1982. Turbulence, transport, and pelagic fish in the California and Peru Current systems. Calif. Coop. Oceanic Fish. Invest. Rep. 23: (this volume).

Barnes, C.A., A.C. Duxbury, and B.-A. Morse. 1972. Circulation and selected properties of the Columbia River effluent at sea. *In* A.T. Pruter and D.L. Alverson (eds.), The Columbia River estuary and adjacent ocean waters. Univ. Wash. Press, Seattle and London, p. 41–80.

Brewer, G.D., and P.E. Smith. 1982. Northern anchovy and Pacific sardine spawning off southern California during 1978-80: preliminary observations on the importance of the nearshore coastal region. Calif. Coop. Oceanic Fish. Invest. Rep. 23: (this volume).

Cannon, G.A., N.P. Laird, and T.V. Ryan. 1975. Flow along the continental slope off Washington, autumn 1971. J. Mar. Res. 33 (Supplement):97–107.

Cullen, J.J. 1981. Chlorophyll maximum layers of the Southern California Bight and mechanisms of their formation and maintenance. Ph.D. dissertation, Scripps Institution of Oceanography, University of California, San Diego, 140 p.

Elsberry, R.L., and R.W. Garwood, Jr. 1978. Sea-surface temperature anomaly generation in relation to atmospheric storms. Bull. Amer. Meteor. Soc. 59(7):786-789.

Garwood, R.W., Jr. 1977. An oceanic mixed layer model capable of simulating cyclic states. J. Phys. Oceanogr. 7(3):455-468.

Hesselberg, Th., and H.U. Sverdrup. 1915. Die Stabilitätsverhältnisse des Seewassers bei vertikalen Verschiebungen. Bergens Museums Aarbok 1914-15, No. 15, 16 p.

Hewitt, R. 1980. Distributional atlas of fish larvae in the California Current region: northern anchovy, *Engraulis mordax* Girard, 1966 through 1979. Calif. Coop. Oceanic Fish. Invest. Atlas 28, vii-xi, charts 1-101.

Hjort, J. 1914. Fluctuations in the great fisheries of northern Europe viewed in the light of biological research. Rapp. P.-v. Réun. Cons. int. Explor. Mer 20:1–228.

———. 1926. Fluctuations in the year classes of important food fishes. J. Cons. int. Explor. Mer 1:5–38.

Kramer, D., and E.H. Ahlstrom. 1968. Distributional atlas of fish larvae in the California Current region: northern anchovy, *Engraulis mordax* Girard, 1951 through 1965. Calif. Coop. Oceanic Fish. Invest. Atlas 9, vii-xi, Charts 1–269.

Kullenberg, G.E.B. 1978. Vertical processes and the vertical-horizontal coupling. *In* J.H. Steele (ed.), Spatial pattern in plankton communities. Plenum Press, New York and London, p. 43–71.

Lasker, R. 1975. Field criteria for survival of anchovy larvae: the relation between inshore chlorophyll maximum layers and successful first feeding. Fish. Bull., U.S. 73(3):453–462.

———. 1978. The relation between oceanographic conditions and larval anchovy food in the California Current: identification of factors contributing to recruitment failure. Rapp. P.-v. Réun. Cons. int. Explor. Mer 173:212–230.

———. 1981a. The role of a stable ocean in larval fish survival and subsequent recruitment. *In* R. Lasker (ed.), Marine fish larvae: morphology, ecology, and relation to fisheries. Univ. Wash. Press, Seattle, p. 80–87.

———. 1981b. Factors contributing to variable recruitment of the northern anchovy *(Engraulis mordax)* in the California Current: contrasting years, 1975 through 1978. Pp. 375–388 *in* R. Lasker and K. Sherman (eds.), The early life history of fish: recent studies. The Second ICES Symposium, Woods Hole, Mass., April 1979. Rapp. P.-v. Réun. Cons. int. Explor. Mer 178.

Lasker, R., H.M. Feder, G.H. Theilacker, and R.C. May. 1970. Feeding, growth and survival of *Engraulis mordax* larvae reared in the laboratory. Mar. Biol. 5:345–353.

Lasker, R., and P.E. Smith. 1977. Estimation of the effects of environmental variations on the eggs and larvae of the northern anchovy. Calif. Coop. Oceanic Fish. Invest. Rep. 19:128–137.

Mais, K.F. 1981. Age-composition changes in the anchovy, *Engraulis mordax*, central population. Calif. Coop. Oceanic Fish. Invest. Rep. 22:82–87.

May, R.C. 1974. Larval mortality in marine fishes and the critical period concept. *In* J.H.S. Blaxter (ed.), The early life history of fish. Springer-Verlag, New York-Heidelberg-Berlin, p. 3–19.

Methot, R.D., Jr. 1981. Growth rates and age distributions of larval and juvenile northern anchovy, *Engraulis mordax*, with inferences on larval survival. Ph.D. dissertation, Scripps Institution of Oceanography, University of California, San Diego, 209 p.

Monahan, E.C. 1971. Oceanic whitecaps. J. Phys. Oceanogr. 1(2):139–144.

Nelson, C.S. 1977. Wind stress and wind stress curl over the California Current. U.S. Dep. Commer., NOAA Tech. Rep. NMFS SSRF-714, 87 p.

Nelson, C.S., and D.M. Husby. In press. Climatology of surface heat fluxes over the California Current region. U.S. Dep. Commer., NOAA Tech. Rep. NMFS SSRF.

Nelson, W.R., M.C. Ingham, and W.E. Schaaf. 1977. Larval transport and year-class strength of Atlantic menhaden, *Brevoortia tyrranus*. Fish. Bull., U.S. 75(1):23–41.

Niiler, P.P., and E.B. Kraus. 1977. One-dimensional models of the upper ocean. *In* E.B. Kraus (ed.), Modelling and prediction of the upper layers of the ocean. Pergamon Press, New York, p. 143–172.

Owen, R.W., Jr. 1968. Oceanographic conditions in the northeast Pacific Ocean and their relation to the albacore fishery. Fish. Bull., U.S. 66(3):503–526.

Parrish, R.H., and A.D. MacCall. 1978. Climatic variation and exploitation in the Pacific mackerel fishery. Calif. Dept. Fish Game, Fish Bull. 167:110 p.

Parrish, R.H., C.S. Nelson, and A. Bakun. 1981. Transport mechanisms and reproductive success of fishes in the California Current. Biol. Oceanogr. 1(2):175–203.

Reed, R.K., and D. Halpern. 1976. Observations of the California Undercurrent off Washington and Vancouver Island. Limnol. Oceanogr. 21(3):389–398.

Reid, F.M.H., E. Stewart, R.W. Eppley, and D. Goodman. 1978. Spatial distribution of phytoplankton species in chlorophyll maximum layers off southern California. Limnol. Oceanogr. 23(2):219–226.

Reid, J.L., Jr. 1973. The shallow salinity minima of the Pacific Ocean. Deep-Sea Res. 20(1):51–68.

Reid, J.L., Jr., G.I. Roden, and J.G. Wyllie. 1958. Studies of the California Current System. Calif. Coop. Oceanic Fish Invest., Prog. Rep., 1 July 1956 to 1 January 1958, p. 27–57.

Richardson, S.L. 1980. Spawning biomass and early life of northern anchovy, *Engraulis mordax*, in the northern subpopulation off Oregon and Washington. Fish. Bull., U.S. 78(4):855–876.

Smith, P.E. 1972. The increase in spawning biomass of northern anchovy, *Engraulis mordax*. Fish. Bull., U.S. 70(3):849–874.

Smith, P.E., L.E. Eber, and J.R. Zweifel. 1981. Large-scale environmental events associated with changes in the mortality rate of the larval northern anchovy. P. 200 *in* R. Lasker and K. Sherman (eds.), The early life history of fish: recent studies. The Second ICES Symposium, Woods Hole, Mass., April 1979. Rapp. P.-v. Réun. Cons. int. Explor. Mer 178.

Smith, P.E., and R. Lasker. 1978. Position of larval fish in an ecosystem. Rapp. P.-v. Réun. Cons. int. Explor. Mer 173:77–84.

Smith, P.E., and S.L. Richardson (eds.) 1977. Standard techniques for pelagic fish egg and larva surveys. FAO Fish. Tech. Pap. 175, 100 p.

Steele, J. 1977. Ecological modelling of the upper layers. *In* E.B. Kraus (ed.), Modelling and prediction of the upper layers of the ocean. Pergamon Press,New York, p. 243–250.

Sverdrup, H.U., M.W. Johnson, and R.H. Fleming. 1942. The oceans: their physics, chemistry and general biology. Prentice Hall, Englewood Cliffs, 1087 p.

Therriault, J.-C., and T. Platt. 1981. Environmental control of phytoplankton patchiness. J. Fish. Res. Bd. Can. 38(6):368–641.

Tibby, R.B. 1941. The water masses off the west coast of North America. J. Mar. Res. 4(2):112–121.

Tully, J.P. 1964. Oceanographic regions and assessment of temperature structure in the seasonal zone of the North Pacific Ocean. J. Fish. Res. Bd. Can. 21(5):941–970.

Vrooman, A.M., P.A. Paloma, and J.R. Zweifel. 1981. Electrophoretic, morphometric, and meristic studies of subpopulations of northern anchovy, *Engraulis mordax*. Calif. Fish Game 67(1):39–51.